JLB

Brief Conclusive Report

Control of the proliferation of activated CD4$^+$ T cells by connexins

Ernesto Oviedo-Orta, Matthieu Perreau,† W. Howard Evans,‡ and Ilaria Potolicchio†,1*

*Faculty of Health and Medical Sciences, University of Surrey, Guildford, United Kingdom; ‡School of Medicine, Department of Infection, Immunity and Biochemistry, Cardiff University, Wales, United Kingdom; and †Laboratory of AIDS, Centre Hospitalier Universitaire Vaudois, Lausanne, Switzerland

RECEIVED SEPTEMBER 14, 2009; REVISED FEBRUARY 23, 2010; ACCEPTED FEBRUARY 27, 2010. DOI: 10.1189/jlb.0909613

ABSTRACT

As expression of Cxs in cells of the immune system increases upon cellular activation, we investigated whether Cxs and especially CxHcs play a major role during T cell-mediated responses. In particular, we studied the expression of Cx43Hc following CD4$^+$ T cell stimulation using flow cytometry, real-time PCR, and Western blot analysis. We showed that expression of Cx43 and its phosphorylated isoforms increased in response to the engagement of CD3 and CD28. Cx43Hcs were found to be involved in sustaining proliferation of T cells, as assessed by cell cycle staining, thymidine incorporation assays, and CFSE analysis of cells exposed to mimetic peptide inhibitors of the plasma membrane Cx channels and antibodies generated to an extracellular region of Cx. The reduction of T cell proliferation mediated by Cx channel inhibitors suppressed cysteine uptake but not cytokine production. We conclude that upon antigen recognition, T cells require CxHc to sustain their clonal expansion. *J. Leukoc. Biol.* 88: 79–86; 2010.

Introduction

Cxs have emerged as important components of the cell communication technology. They function as hexameric Hcs at unopposed regions of the cell surface or as dodecameric "double" channels that comprise gap junction plaques. Over 20 Cxs are found in human and mouse genomes, and as cells often express more than one Cx type, channels may be homomeric or heteromeric [1].

Gap junction channels and CxHcs differ: Gap junction channels are open, whereas CxHcs are unattached, single channels but may open under conditions of stress (e.g., osmotic, mechanical, ischemic). Gap junctions are strongly adhesive double channels, whereas CxHcs are unattached channels. Lastly, gap junctions connect the cytoplasms of adjacent cells directly, whereas CxHcs, in open configuration, link the cytoplasm with the outside milieu. Both structures can allow intercellular signaling. Molecular/ionic trafficking through CxHc has been easier to analyze and includes ATP, Ca^{2+}, cAMP, NAD, glucose, glutathione, and glutamate [2].

Gating of Cx channels is poorly understood but may involve interaction of the cytoplasmic loop with the carboxyl tail [3]. Although the precise mechanism by which CxHcs are regulated is unclear, one possibility is that phosphorylation of amino acids in the cytoplasmic tail may play a key role [4–6].

Cx40 and Cx43 are widely expressed by cells of the immune system with monocytes, DCs, and NK, B, and T cells expressing these Cxs on their plasma membrane [7, 8]. Up-regulation of Cx expression by proinflammatory molecules such as LPS or IFN-γ has been reported [9]. Cx-based gap junction communication is involved in peptide antigen transport between DCs, a mechanism that is likely to participate in antigen cross-presentation [10]. Gap junctions are also implicated in leukocyte transmigration across the endothelium, in secretion of cytokines and Igs, and in cross-talk between macrophages and lymphocytes [11–13].

The purpose of this study was to investigate the role of CxHc in CD4$^+$ T cells following cell stimulation. Our results show that a reorganization of CxHc expression occurred upon T cell activation. This is possibly related to a role that CxHcs play in sustaining T cell proliferation.

MATERIALS AND METHODS

Cell culture and flow cytometry

PBMC from healthy donors were prepared by Ficoll-Hypaque density gradient centrifugation. RPMI 1640 supplemented with L-glutamine, antibiotics, 20 mM Hepes, and 10% FCS was used in all in vitro assays. CD4$^+$CD25$^-$ T cells were sorted prior to analysis with mouse anti-human CD4-PerCy5 (BD Bioscience, San Jose, CA, USA) and CD25$^-$ allophycocyanin (BD Bioscience) antibodies. For intracellular staining of Cx43, CD4$^+$CD25$^-$ T cells were treated with Cytofix/Cytoperm (BD Bioscience) prior to staining and analysis by flow cytometry. Mouse anti-human CD3 antibody (clone UCHT1; BD PharMingen, San Diego, CA, USA) and mouse anti-human CD28 antibody (BD PharMingen) were used to stimulate lymphocytes in vitro. Immunoprecipitation was performed using a rabbit anti-Cx43 anti-

Abbreviations: Cx=connexin, CxHc=connexin hemichannel, DC=dendritic cell, EL-1=first extracellular loop, Hc=hemichannel, LAT=linker for activation of T cell, TT=tetanus toxoid

1. Correspondence: Service d'Immunologie et d'Allergie (IAL), DM-CHUV (Centre Hospitalier Universitaire Vaudois), Ave Beaumont 29, Room BT02-252, Lausanne 1011, Switzerland. E-mail: ilaria.potolicchio@chuv.ch

body (clone C6219; Sigma Chemical Co., St. Louis, MO, USA). We used BD Imag™ anti-human CD8 particles (BD Bioscience) to isolate $CD8^+$ T cells.

The following antibodies were used: rabbit anti-human phospho-Cx43 (Ser368; Cell Signaling, Beverly, MA, USA), anti-phosphotyrosine 4G10 (Millipore, Bedford, MA, USA), mouse anti-Cx43 (clone CX-1B1; Zymed, San Francisco, CA, USA), rabbit anti-Cx43 (Zymed), rabbit anti-Cx43 (Sigma Chemical Co.), and rabbit Gap7M, a polyclonal antibody that recognizes the EL-1 of several Cxs [14, 15]. We used the following secondary antibodies: Fab goat anti-rabbit Alexa Fluor® 633 or Alexa Fluor® 488 and Fab goat anti-mouse Alexa Fluor® 633 or Alexa Fluor® 488 (Molecular Probes, Eugene, OR, USA). For all of the experiments, we used isotype controls or 1% of a commercially available rabbit serum.

Immunogold labeling of ultrathin cryosections

$CD4^+$ T cells were fixed in a mixture of 2% paraformaldehyde in phosphate buffer 0.2 M, pH 7.4, at 4°C. Fixed cells were processed for ultrathin cryosectioning as described previously [16]. Immunogold labeling was performed using a rabbit anti-Cx43 (Zymed) in combination with Protein A coupled to 10 nm or 15 nm gold particles. Contrast was obtained with a mixture of 2% methylcellulose (Sigma Chemical Co.) and 0.4% uranyl acetate pH 4 (EMS, Hatfield, PA, USA). Samples were viewed under a CM10/CM12 Philips electron microscope (Eindhoven, The Netherlands).

Real-time RT-PCR

Cells were stimulated for 1 h with an anti-CD3 antibody-coated plate and soluble anti-CD28 antibody. RNA from unstimulated or stimulated $CD4^+$ T cells was prepared using a RNAeazy (Qiagen, Valencia, CA, USA) and RT carried out using a QuantiTect RT kit (Qiagen). The resulting cDNAs were submitted to quantitative real-time PCR analysis. We used a human KIAA1432 gene (Qiagen) to amplify the Cx43 and human RRN18S (18S rRNA; Qiagen) as a control gene. SYBR Green PCR master mix (Qiagen) was used in PCR reactions. We used an ABI PRISM® 7700 sequence detection system programmed as follows: an initial step of 2 min at 50°C and 10 min at 95°C, followed by 40 cycles of 10 s at 95°C and 1 min at 60°C. Each reaction was performed in duplicate. Amplification of Cx43 was calculated using the spreadsheet for the Pfaffl equation [17], available on line (http://pathmicro.med.sc.edu/pcr/pcr-pfaffl.htm).

Stimulation of T cells for Western blot analysis and ELISA

Purified $CD4^+CD25^-$ cells were stimulated overnight with anti-CD3 antibody and soluble anti-CD28 antibody as described. Untreated T cells were analyzed in parallel with stimulated T cells. For Western blot analysis of plasma membrane-associated Cx43, cell-surface biotinylation was performed using EZ-link sulfo-NHS-SS-biotin (Pierce, Rockford, IL, USA). Biotinylated cells were lysed at room temperature in 0.2% of SDS-TBS buffer (pH 8.0) containing a mixture of protease inhibitors (Roche Applied Science, Indianapolis, IN, USA). After protein extraction and quantification, samples were diluted tenfold and 30 mg-immunoprecipitated and captured on protein G-Sepharose (Sigma Chemical Co.). Samples were washed with 1% Triton X-100/TBS and resuspended in 800 μl TBS. Four hundred microlitres were incubated with alkaline phosphatase for 1 h at 37°C as described previously [18], diluted in Laemmli sample buffer, and resolved by SDS-PAGE in nonreducing conditions. Streptavidin-HRP (BD Pharmingen) was used as a detection method, and ECL, using West Pico chemiluminescent substrate (Pierce), was used to visualize the reaction. Otherwise, cells were lysed and added to an ELISA plate coated previously with rabbit anti-Cx43 (Sigma Chemical Co.). The analysis was done in triplicate using a JASCO CD (Easton, MD, USA) spectrometer for densitometric analysis.

T cell proliferation assay

Polyclonal activation of $CD4^+CD25^-$ T cells (5×10^5) was performed using 1 μg/ml soluble CD3 antibody and 0.5 μg/ml soluble CD28 antibody. Irradiated PBMC were used as feeder cells (2×10^5), which were cultured for 5 days with or without Gap27 (amino acid sequence SRPTEKTIFII) mimetic peptide designed from the EL-2 of Cx43. Cells were cultured in parallel with the scrambled Gap27 peptide (SITIRFTPEKI) used as a control. T cell proliferation was assessed by ^{3}H-thymidine incorporation during the last 16–18 h of culture. We used 100 μg/ml TT (Aventis Pasteur, Lyon, France) to assess antigen-specific T cell responses. Autologous PBMC (2.5×10^5) were prepulsed with TT for 12 h and then irradiated and incubated for 5 days with TT-specific $CD4^+$ T cells (in-house-generated cell line from a healthy donor; 5×10^5). Proliferation was assessed by ^{3}H-thymidine incorporation during the last 16–18 h of culture. In related experiments, isolated $CD4^+$ or $CD8^+$ T cells were stimulated with magnetic beads coated with anti-CD3/CD28 antibodies (Dynabeads, Invitrogen, Carlsbad, CA, USA) and cultured for 5 days in the presence or absence of 10 μg/ml Gap7M. We also used 100 μM oleamide (donated by Prof. Paolo Meda, University of Geneva, Switzerland) as a chemical inhibitor of CxHc [19]. Proliferation was also assessed by CFSE staining (Molecular Probes, Invitrogen). Cells were CFSE-stained prior to stimulation with anti-CD3/CD28-coated magnetic beads. Gap7M was used as described above, and cells were analyzed by flow cytometry after 5 days in culture. Rabbit serum was used as control.

Cell cycle analysis

Cells were activated in vitro for 72 h as described above and cell pellets collected by centrifugation and fixed in ethanol for 1 h at 4°C. Samples were incubated with RNase, 2 mg/ml, and propidium iodide, 5 μg/ml (Sigma Chemical Co.), for 15 min at 4°C. DNA content was measured using FACScan flow cytometer (Becton Dickinson, San Diego, CA, USA). Histograms of cell numbers versus linear-integrated red fluorescence were recorded. Cell cycle analysis was obtained by a FlowJo program.

Statistical analysis

Unless otherwise stated, all experiments were carried out in triplicate. Values are expressed as mean ± SD. A paired Student's *t*-test analysis between samples and controls was performed using GraphPad Prism (Version 5.01). Values of $P < 0.05$ were considered significant.

Cytokine analysis

Cytokine synthesis was measured by flow cytometry as described previously [20]. Briefly, $CD4^+CD25^-$ T cells were incubated overnight with 1 μg/ml GolgiPlug reagent (BD Bioscience) in the presence of anti-CD3/CD28-coated magnetic beads (Invitrogen). Cells were then fixed and permeabilized with BD Cytofix/Cytoperm solutions (BD Bioscience). Intracellular staining of IFN-γ and IL-2 was performed using anti-human IFN-γ-allophycocyanin- and IL-2-PE-labeled antibodies (BD Pharmingen). Alternatively, cells were cultured for 2 days and supernatants collected for analysis of cytokine synthesis using a semiquantitative human cytokine array kit (R&D Systems, Minneapolis, MN, USA).

Cysteine transport assay

T cells (1×10^6 cells) were stimulated using magnetic beads coated with CD3/CD28 antibodies (Dynabeads, Invitrogen) or with 10 μg/ml Gap7M antibody. Untreated and stimulated $CD4^+$ T cells were collected and washed with PBS/2 mM EDTA, pH 8.0, after 12 and 48 h, and cell pellets were transferred into a reducing, cysteine-free cell culture medium (Gibco, Grand Island, NY, USA) containing 10% dialyzed FCS and 0.02% β2-ME. Amino acid transport activity was measured by incubating the samples with 0.5 μCi/ml cysteine-[S^{35}] for 20 min at 37°C. Gap7M was added a few minutes before cysteine [S^{35}]. T cells were washed four times in Hanks' saline buffer (Gibco) and protein extracts quantified using a spectrophotometer. Equal amounts of proteins were transferred onto a 96-well microplate (Millipore) and radioactivity uptake measured in a MicroBeta microplate scintillation counter (PerkinElmer Life Science, Boston, MA, USA).

RESULTS AND DISCUSSION

Cxs are expressed mainly at the surface of most animal cells, as hexameric Hcs that migrate laterally for recruitment into edges of gap junctions. Murine T lymphocytes up-regulate Cx31.1, Cx32, Cx43, and Cx46 upon activation [21].

Cx43 is expressed at the plasma membrane of resting T lymphocytes (**Fig. 1A**). In $CD4^+$ T cells, the expression of Cx43 increases after treatment with PHA-L [22], but functional aspects during immune responses remain to be established. To address this question, we investigated whether the expression of Cx43 was linked directly to the activation of the TCR. $CD4^+CD25^-$ T cells were sorted and then stimulated using anti-CD3 and anti-CD28 antibodies. We used real-time PCR to analyze the expression of Cx43 mRNA in resting and stimulated $CD4^+$ T cells using 18S RNA as a control. The increased expression of Cx43 in stimulated $CD4^+$ T cells was calculated applying the Pfaffl method [17], which allowed us to determine the relative expression ratio between the sample (Cx43 mRNA) and the calibrator (18S mRNA) in stimulated versus unstimulated $CD4^+$ T cells (Fig. 1B). The expression of Cx43 was found to be 2400 times higher in stimulated $CD4^+$ T cells than in unstimulated cells. An increase in the number of cells expressing Cx43 correlated with an up-regulation of the expression of CD69, a classic activation marker of T cells. After 48 h of T cell stimulation with CD3/CD28 antibodies, only $CD4^+CD69^+$ T cells up-regulated Cx43 (Fig. 1C).

With the exception of Cx26, there is strong evidence that the activity of the CxHc is controlled by protein kinase-induced phosphorylation events [23]. We therefore studied the effects of CD3/CD28 stimulation on the phosphorylation status of Cx43. Phosphorylation of Cxs occurs mainly on serine residues on the protein cytoplasmic tail [24], although tyrosine phosphorylation has also been reported [25]. We studied Cx43 phosphorylation by flow cytometry with a mAb that recognizes the Ser368-phosporylated residue using permeabilized, unstimulated, and stimulated $CD4^+$ T cells. Activated $CD4^+$ T cells showed increased Ser368 phosphorylation compared with resting T cells. Rabbit serum was used as a negative control (**Fig. 2A**). An increase in Cx phosphorylation was also observed in stimulated $CD4^+$ T cells by ELISA when a polyclonal antibody specific to Cx43 was used as capture antibody (Fig. 2B). The phosphorylated Cx43 component was analyzed using an antibody 4G10, specific for phosphotyrosines. Finally, phosphorylation of Cx43 expressed at the cell surface of stimulated and unstimulated $CD4^+$ T lymphocytes was analyzed by Western blotting. Cell surface-exposed proteins were biotinylated and Cx43-immunoprecipitated with a polyclonal antibody to a sequence in the cytoplasmic tail of Cx43. Identical amounts of protein extracted from cell pellets were subjected to affinity chromatography, and the entire protein yield was run on a gel. Two Cx43 isoforms were observed by SDS-PAGE (Fig. 2C, lanes 1 and 2). Alkaline phosphatase treatment removed the slower migrating isoform that corresponded to the phosphorylated form of Cx43 (Fig. 2C, lane 3).

Taken together, these data demonstrate that Cx43 expression is up-regulated in response to the CD3/CD28 engagement and that T cell activation also results in increased phosphorylation of Cx43. Channel permeability or stringency to different solutes may be decreased or increased by phosphorylation of Cx43 [23]. The effect of the phosphorylation in controlling the gating system of the Hcs is residue-specific. It was not possible to discern a specific function associated with the Cx43 phosphorylation during T cell activation, as there are phosphorylation sites.

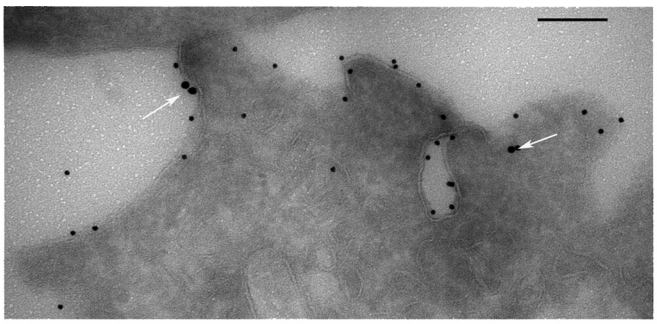

B

Equation 1: Deviation of target gene $(E_{tar.})=1.93^{Cx43\ (unt-stim)\ CD4}=1.93^{13.03}=5474.91$
Equation 2: Deviation of reference gene $(E_{ref.})=1.93^{18S\ (unt-stim)\ CD4}=1.93^{1.23}=2.26$
Equation 3: Time fold increase in Cx43 gene expression Ratio= $(E_{tar.})$ / $(E_{ref.})$ = **2418.6**

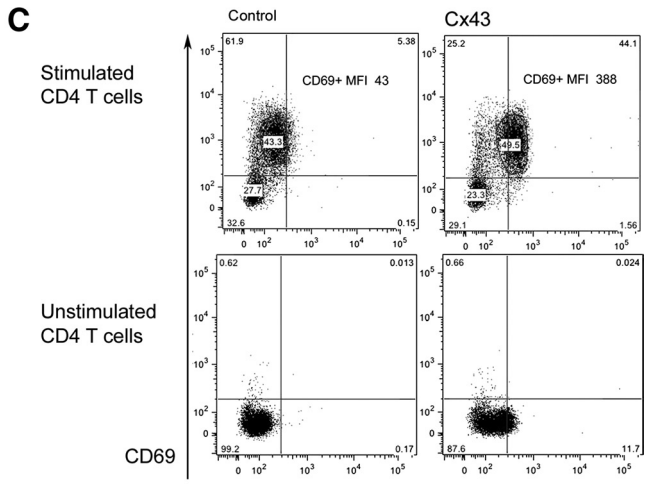

Figure 1. Expression of Cx43 by $CD4^+$ T lymphocytes. (A) Ultrastructural analysis of $CD4^+$ T cells showing cell surface expression of Cx43, 15 nm gold particles (white arrows), and CD3, 10 nm gold particles. (B) Analysis of the expression of Cx43 mRNA [target gene $(E_{tar.})$] and 18S RNA subunit [reference gene $(E_{ref.})$] in stimulated and unstimulated $CD4^+$ T cells using the Pfaffl mathematical formula. (C) Characterization of the expression of CD69 and Cx43 by stimulated $CD4^+$ T cells (upper right panel) and unstimulated $CD4^+$ T cells (lower right panel). Nonimmune rabbit serum was used as control (upper and lower left panels). MFI, Mean fluorescence intensity.

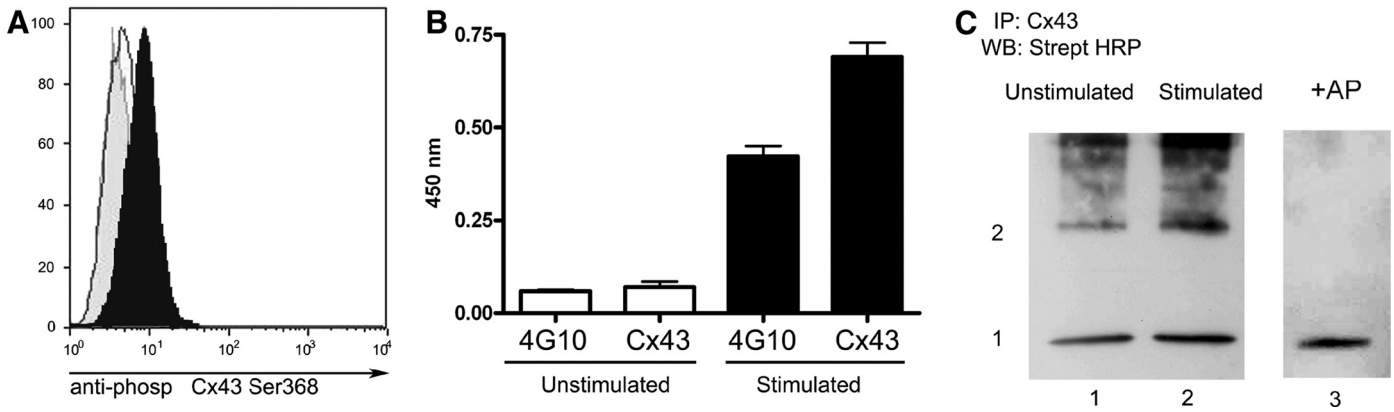

Figure 2. Effect of CD3/CD28 stimulation on Cx43 phosphorylation status in $CD4^+$ T cells. Lymphocytes were stimulated in vitro by magnetic beads coated with CD3 and CD28 antibodies. (A) Flow cytometry analysis using phosphotyrosine Cx43 Ser368 antibody. The histogram shows the effect of stimulation on $CD4^+$ T cells (black curve) versus unstimulated cells (open white curve) and negative control (gray curve). (B) Semiquantitative ELISA analysis of Cx43 expressed by unstimulated and stimulated $CD4^+$ T cells. Detection of Cx43-phosphorylated isoforms used mAb 4G10; total Cx43 proteins expressed used CX-1B1 antibody (see Materials and Methods). Absorbance was measured at 450 nm, and values are expressed as absorbance units. The panel shows a representative experiment. (C) Assessment of immunoprecipitated (IP) Cx43 by Western blot (WB) analysis. Lymphocyte plasma membranes were biotinylated and 30 mg of a total protein extract loaded onto a Cx43 affinity column. The protein yield was analyzed by SDS-PAGE gel: lane 1, unstimulated $CD4^+CD25^-$ T cells; lanes 2 and 3, stimulated $CD4^+CD25^-$ T cells. Lane 3 treatment was with alkaline phosphatase (AP). Streptavidin (Strept)-HRP was used for detection.

Cx43-Hcs play a role in T cell proliferation

Cell growth requires the uptake of nutrients acquired from the extracellular environment. These, in turn, control the proliferation of T cells [26]. In extracellular oxidizing environments, free cysteine is converted rapidly into the disulfide-bonded form. T cells require a reducing environment to proliferate, as their cysteine uptake is limited to the thiolic forms [27, 28]. Macrophages and DCs control T cell-mediated responses according to the availability of cysteine and tryptophan for T cell proliferation [29]. Thus, changes in cell membrane permeability implicating Cx channels might influence the proliferation of T lymphocytes. We examined the effects of CxHc inhibitors during T cell proliferation. As expected, $CD4^+CD25^-$ T cells responded with a high rate of T cell proliferation when cultured in the presence of feeder cells along with soluble CD3 and CD28 antibodies (**Fig. 3A**). However, in the presence of Gap27, a Cx mimetic peptide that blocks CxHc [30] proliferation of $CD4^+$ T cells was reduced in a dose-dependent manner (Fig. 3A). This mimetic peptide is likely to interact with the second extracellular domain of membrane-associated Cxs [30] and blocks ATP release and Ca^{2+} entry [12]. A scrambled control mimetic peptide had little effect on $CD4^+$ T cell proliferation (Fig. 3A). Similarly, Gap27 but not the scramble peptide inhibited T cell proliferation following antigen-specific stimulation with TT (Fig. 3B). In this experiment, autogenic PBMC were pulsed with the TT for 12 h prior to irradiation and coculturing with TT-specific $CD4^+$ T cells. As expected, antigen-specific $CD4^+$ T cells did not proliferate without the addition of the TT when cocultured with the autogenic, irradiated PBL (Fig. 3B). Thus, in both systems, polyclonal and antigen-specific stimulation, the proliferation of the $CD4^+$ T cells was inhibited by Cx channel inhibitors. To address the question of whether the mimetic peptide was interfering with the formation of gap junctions between T cells and APC, the experiments were repeated in the absence of feeder cells and stimulating the $CD4^+$ T cells with magnetic beads coated with anti-CD3 and anti-CD28 antibodies (Fig. 3, C and D). We used two different inhibitors: Gap7M, which is a generic polyclonal antibody that binds to the second extracellular loop of CxHc but not to gap junctions [14], and the oleamide, a generic inhibitor of gap junction communication [31]. The inhibitory effect of the polyclonal antibody was studied by flow cytometry (Fig. 3C). CFSE-labeled $CD4^+$ T cells were stimulated and the proliferation rate determined by CFSE dilution after 5 days in culture (Fig. 3C). Unstimulated $CD4^+$ T cells were analyzed in parallel (Fig. 3C). T cell proliferation was inhibited by Gap7M (Fig. 3C). Cell viability was found to be approximately 98%, showing that inhibitory effects on T cell proliferation were not a result of cell death. Furthermore, when proliferation was analyzed at 72 h, the proliferation rate in stimulated $CD4^+$ T cells was 40–50%, whereas the proliferation of T cells incubated with Gap7M was ~2% (data not shown). We conclude that Gap7M does not cause production of death signals and that cells exposed to this antibody progress into cell cycle arrest.

Next, we analyzed the effect of oleamide on T cell proliferation. $CD4^+$ and $CD8^+$ T cells (Fig. 3D) were stimulated for 5 days with magnetic beads coated with anti-CD3 and anti-CD28 antibodies and cultured in the presence of Gap7M, oleamide, and 0.5% of DMSO (Fig. 3D). Oleamide and Gap7M antibody inhibited $CD4^+$ and $CD8^+$ T cell proliferation (*, $P<0.05$). Our results indicate that gap junction inhibitors can abrogate the proliferation of the T cells by interfering with the activity of CxHc on the cell surface and not by altering gap junction communication between T cells and APC.

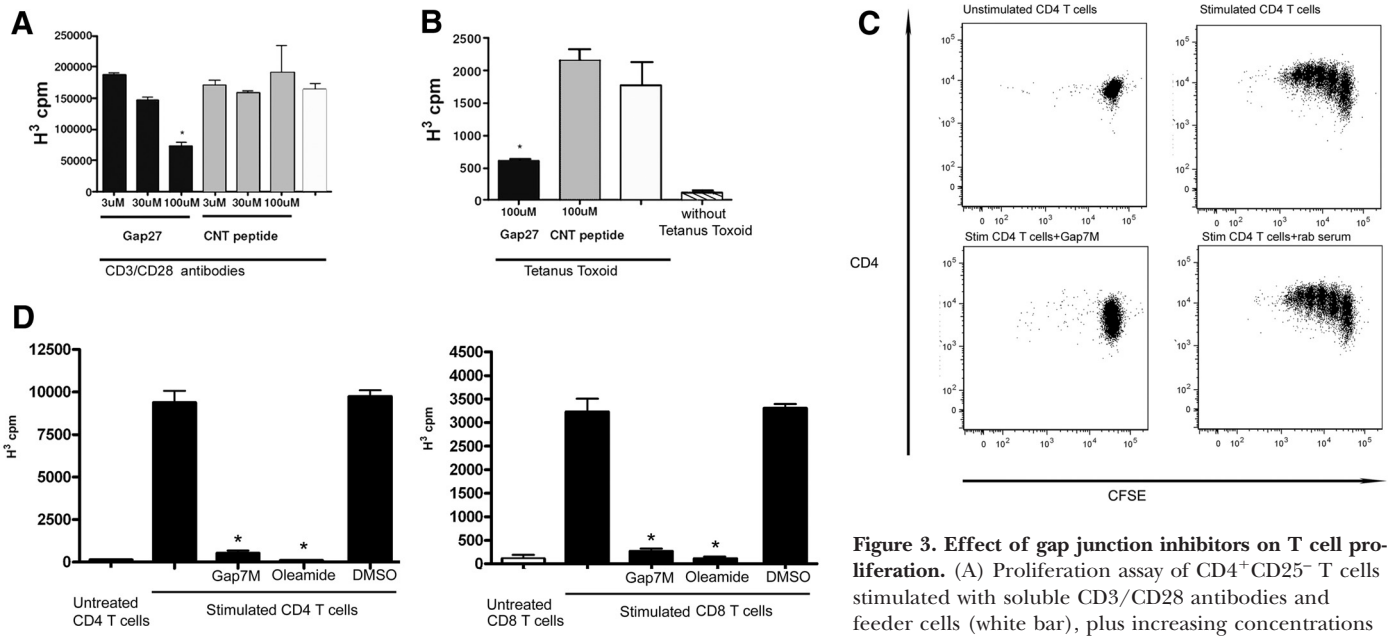

Figure 3. Effect of gap junction inhibitors on T cell proliferation. (A) Proliferation assay of $CD4^+CD25^-$ T cells stimulated with soluble CD3/CD28 antibodies and feeder cells (white bar), plus increasing concentrations of Gap27, a Cx mimetic peptide (black bars), plus increasing concentrations of control scramble (CNT) peptide (gray bars). Cells were cultured for 5 days, and ^3H incorporation was measured after 16 h. Each bar corresponds to the average values obtained from three independent experiments (*, $P<0.05$). (B) Proliferation assay of TT-specific $CD4^+$ T cells stimulated with 100 μg/ml TT and autogenic feeder cells (white bar), plus 100 μM Gap27 (black bar), plus 100 μM control scramble peptide (gray bar) or without the addition of the TT (hatched bar). Cells were cultured for 5 days and ^3H incorporation measured after 16 h. Each bar corresponds to the average values obtained from three independent experiments (*, $P<0.05$). (C) Representative flow cytometry dot blot analysis showing the inhibitory effect of Gap7M antibody on $CD4^+CD25^-$ T cell proliferation in the absence of feeder cells. CFSE-labeled cells were stimulated using magnetic beads coated with CD3/CD28 antibodies and cultured for 5 days. Upper left panel shows control, unstimulated T cells; upper right panel shows T cells stimulated with anti-CD3/CD28; lower left panel shows stimulated T cells incubated in the presence of Gap7M; and lower right panel shows stimulated T cells plus 1% rabbit nonimmune serum. (D) Effect of antibody Gap7M on the proliferation of $CD4^+$ and $CD8^+$ T cells, which were cultured with magnetic beads coated with CD3/CD28 antibodies in the presence of 10 μg/ml Gap7M or 100 μM oleamide. In a separate reaction, 0.5% of DMSO was used as control. Cells were cultured for 5 days, and ^3H incorporation was measured after 16 h. Each bar corresponds to the average values obtained from three independent experiments (*, $P<0.05$).

Cell cycle kinetics was monitored by flow cytometry. After 72 h, $CD4^+$ T cells stimulated with magnetic beads coated with anti-CD3/CD28 antibodies showed a progression into the S and G2/M phases (**Fig. 4A**), as reported previously by others [32, 33]. The percentage of cells found in the G0/G1 phase was significantly higher when $CD4^+$ T cells were stimulated in the presence of Gap7M (Fig. 4A). The percentage of stimulated $CD4^+$ T cells found in G0/G1, S, and G2/M was taken as a reference and the values compared with those obtained from cultures containing Gap7M. We estimated the number of apoptotic cells by evaluating the pre-G0/G1 peak component between stimulated T cells and stimulated T cells incubated with Gap7M. After 48 h and 72 h in culture, there were no significant differences in the percentages of apoptotic cells between the groups. We then investigated the effect of Gap7M on IL-2 and IFN-γ production. IL-2- and IFN-γ-producing $CD4^+$ T cells were measured after overnight stimulation with anti-CD3/CD28-coated magnetic beads (Fig. 4B). Interestingly, Gap7M did not inhibit the production of IL-2 and IFN-γ from CD3/CD28-stimulated $CD4^+$ T cells, probably as after short-term stimulation, IL-2 and IFN-γ are likely to be derived from pre-formed stores rather than by ex novo synthesis. Therefore, we analyzed the production of other cytokines using a human cytokine array kit (see Materials and Methods). The addition of Gap7M did not affect the secretion of inflammatory cytokines, as it showed a similar profile to that of stimulated $CD4^+$ T cells, except for IL-17 secretion, which increased in cells incubated with Gap7M (Fig. 4C). We conclude that Gap7M inhibits the proliferation of T cells selectively but has little effect on the secretion of lymphokines. A similar mechanism has been described in cell–cell contact between alveolar macrophages, which are also able to inhibit the proliferation of activated T cells without interfering with Ca^{2+} flux, IL-2, and IFN-γ secretion [34].

Cysteine uptake in activated $CD4^+$ T cells is compromised by Gap7M extracellular loop antibody

Resting and stimulated T cell clones and T cell-derived tumors are known to have strong cysteine, alanine, and arginine transport activities but little or no transport activity for cystine and glutamate [35]. Moreover, DNA synthesis, measured by H^3-thymidine incorporation, correlates positively with the levels of extracellular cysteine [35]. We therefore analyzed the extracellular uptake of cysteine in stimulated $CD4^+CD25^-$ T cells incubated in the presence of Gap7M. Cells were stimulated by anti-CD3/CD28 beads for 12 h (**Fig. 5A**) and 48 h (Fig. 5A), and intracellular accumulation

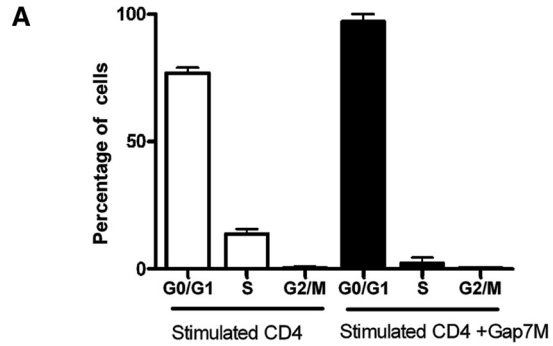

72 h	Stimulated CD4 T cells		Stimulated CD4 T cells +Gap7M		P·
Group	Mean 1	N1	Mean 2	N2	
G0/G1	+ 76.80	3	+ 97	3	<0.05
S	+ 13.77	3	+ 2.20	3	< 0.05
G2/M	+ 0.60	3	+ 0.30	3	ns

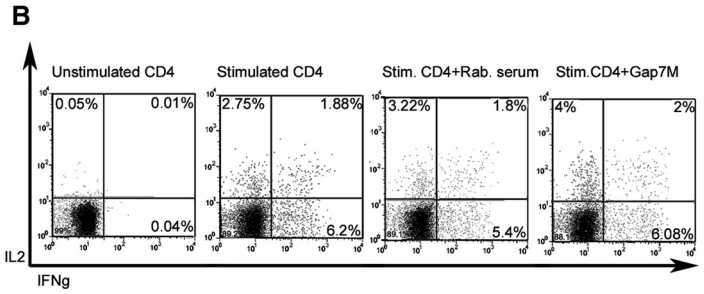

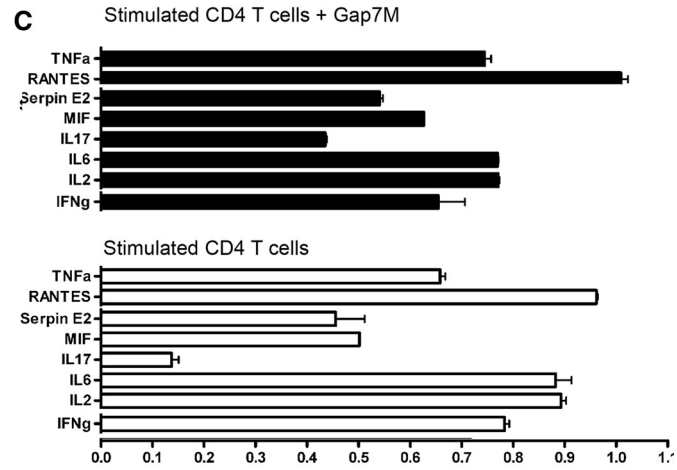

Figure 4. Effect of Cx Gap7M on the cell cycle progression and on secretion of cytokines in CD4$^+$ T cells. (A) A cytofluorimetric cell cycle analysis was performed to detect the proportion of stimulated CD4$^+$ T cells (open bars) versus stimulated CD4$^+$ T cells cultured with Gap7M (black bars). The results of this analysis are given in the table, and the values correspond with the mean values of three independent experiments. (B) Flow cytometry profiles of the secretion of IL-2 and IFN-γ in unstimulated, stimulated, and stimulated CD4$^+$ T cells in the presence of 10 μg/ml Gap7M. Rabbit nonimmune serum was used as a negative control. (C) Detection of cytokine profile secreted by CD4$^+$ T cells cultured in the presence or in the absence of 10 μg/ml Gap7M after 48 h incubation. Cytokine secretion was assessed using R&D Human Cytokine Proteome Profiler™ array. MIF, Migration inhibitory factor.

of [S^{35}]-labeled cysteine in unstimulated (Fig. 5A) and stimulated CD4$^+$ T cells (Fig. 5A) was compared after a 20-min incubation in media containing the radiolabeled amino acid under reducing conditions. A significant inhibition of uptake of [S^{35}]-cysteine (*, $P<0.05$) was observed in the CD4$^+$ T cell after stimulation for 48 h with Gap7M (Fig. 5A). When the antibody was added at the end of the assay, prior to the addition of [S^{35}]-cysteine, the inhibitory effect of Gap7M on unstimulated CD4$^+$ T cells (Fig. 5B) continued but not in stimulated CD4$^+$ T cells (Fig. 5C). These experiments allow two conclusions: 1) As unstimulated CD4$^+$ T cells are nonproliferating, the inhibitory effect of Gap7M on the accumulation of cysteine is likely to be a result of the interaction of the antibody with the externally exposed epitope; 2) in stimulated T cells, the epitope to which Gap7M binds becomes less accessible. We examined the second conclusion further by staining unstimulated and stimulated CD4$^+$ T cells with Gap7M. Cell surface staining showed a reduction in Cx expression after CD3/CD28 T cell stimulation, whereas increased staining was observed with permeabilized cells (Fig. 5D). Thus, Cxs were retained intracellularly in response to the CD3/CD28-mediated activation, or the extracellular loop recognized by the antibody had become hidden upon T cell activation. Gap7M binds to an epitope in the first extracellular loop spanning residues 43–59. This Cx43 domain contains Cys^{54}, which forms an intramolecular disulfide bond with Cys^{192}, positioned in the second extracellular loop [36]. We speculate that binding of Gap7M precludes the interaction Cys^{54}–Cys^{192}, thus interfering with Hc operation.

The studies using Gap7M point to a connection between the Hc function and cysteine movement across the plasma membrane of T cells. Whether Cxs are involved directly in cysteine uptake, or its inhibition is a secondary effect caused by the inhibition of the movement of other molecules is an open question. Nevertheless, it is important to highlight the possibility that Cxs and other plasma membrane Hcs, such as those formed by pannexins, may also play in lymphocyte T cell proliferation.

Finally, we examined the effects of Gap7M on amino acid transporters. Amino acids are transported across the lymphocyte's plasma membrane by the transport system L, formed by a common heavy chain CD98, bound to different light chains. Cysteine uses the light chain LAT2. CD98 was described first as one of the lymphocyte activation markers [37] and is expressed in different cell types [38]. We studied the expression of CD98 by flow cytometry in activated CD4$^+$ T cells in the presence of Gap7M and found that Cx43 was still highly expressed in the presence of Gap7M (Fig. 5E). Thus, the inhibitory effect of Gap7M is likely to be a result of interaction with its epitope in the first extracellular loop and not a result of the lack of Lats at the cell surface. A similar effect of Gap7M was reported recently in

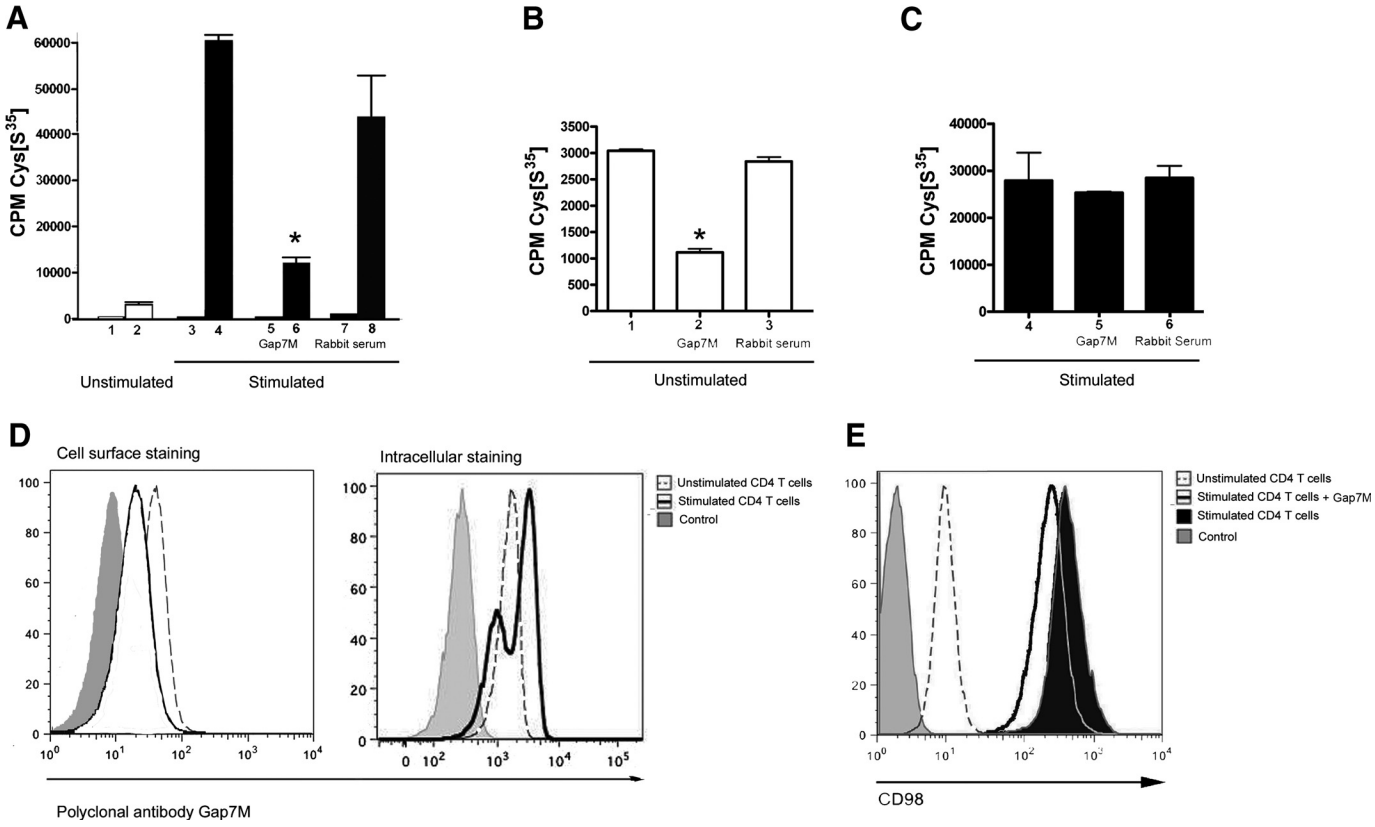

Figure 5. Inhibition of Cys-[S^{35}] uptake in cells treated with Gap7M antibody. (A) CD4$^+$CD25$^-$ T cells were stimulated for 12 h (bars 1, 3, 5, 7) or 48 h (bars 2, 4, 6, 8) with magnetic beads coated with CD3/CD28 antibodies. Accumulation of Cys-[S^{35}] is reported as cpm/10 μg proteins. Bars 5 and 6 represent data collected from cells stimulated for 48 h in the presence of Gap7M (*, $P<0.05$). (B and C) The results gathered from unstimulated and stimulated CD4$^+$ T cells cultured for 48 h, respectively (*, $P<0.05$). Bars 1 and 4 show the Cys-[S^{35}] uptake levels by unstimulated and stimulated CD4$^+$ T cells. Bars 2 and 5 show Cys-[S^{35}] uptake in unstimulated and stimulated CD4$^+$ T cells plus Gap7M antibody, and bars 3 and 6 show results obtained from unstimulated and stimulated CD4$^+$ T cells incubated with nonimmune rabbit serum. (D) Flow cytometry analysis of the effects of Gap7M on the cell surface (left panel) or intracellular expression (right panel) of Cxs. Untreated CD4$^+$ T cells (dashed lines) were compared with stimulated cells (continuous lines). Rabbit serum was used as control (gray curves). (E) Flow cytometry analysis of the expression of CD98 in unstimulated (dashed line) and stimulated CD4$^+$ T cells with (continuous line) or without (black curve) Gap7M. An isotype antibody was used as negative control (gray curve).

which this antibody inhibited Ca^{2+} oscillations and Ca^{2+} uptake by cardiac cells [39].

In conclusion, our results show that by modulating the expression of CxHc, T cells regulate the exchange of nutrients and other molecules. During T cell-mediated responses, the CxHcs are required to sustain the proliferation and therefore, the clonal expansion of activated T cells. This is particularly relevant in scenarios where viral proteins of the herpes virus HSV-2 and the human papilloma virus HPV-16 are able to close gap junctions of infected cells [40]. In this regard, it would be interesting to investigate whether other viruses might block CxHc and thus, control T cell proliferation, thereby evading immune surveillance.

AUTHORSHIP

I. P. designed and performed research, analyzed data, and wrote the paper; M. P. performed flow cytometry experiments; E. O-O. provided Gap7M, contributed to data analysis, and wrote the paper; and W. H. E. participated in critical discussion and writing.

ACKNOWLEDGMENTS

We thank Prof. Giuseppe Pantaleo for his support and helpful discussions. We thank Prof. Paolo Meda for supplying the oleamide.

DISCLOSURE

The authors have declared no conflict of interest.

REFERENCES

1. Evans, W. H., De Vuyst, E., Leybaert, L. (2006) The gap junction cellular internet: connexin hemichannels enter the signaling limelight. *Biochem. J.* **397,** 1–14.
2. Evans, W. H., Leybaert, L. (2007) Mimetic peptides as blockers of connexin channel-facilitated intercellular communication. *Cell Commun. Adhes.* **14,** 265–273.
3. Liu, F., Arce, F. T., Ramachandran, S., Lal, R. (2006) Nanomechanics of hemichannel conformations: connexin flexibility underlying channel opening and closing. *J. Biol. Chem.* **281,** 23207–23217.
4. Retamal, M. A., Schalper, K. A., Shoji, K. F., Bennett, M. V., Saez, J. C. (2007) Opening of connexin 43 hemichannels is increased by lowering intracellular redox potential. *Proc. Natl. Acad. Sci. USA* **104,** 8322–8327.
5. Moreno, A. P., Lau, A. F. (2007) Gap junction channel gating modulated through protein phosphorylation. *Prog. Biophys. Mol. Biol.* **94,** 107–119.

6. Ek-Vitorin, J. F., King, T. J., Heyman, N. S., Lampe, P. D., Burt, J. M. (2006) Selectivity of connexin 43 channels is regulated through protein kinase C-dependent phosphorylation. *Circ. Res.* **98,** 1498–1505.
7. Oviedo-Orta, E., Howard Evans, W. (2004) Gap junctions and connexin-mediated communication in the immune system. *Biochim. Biophys. Acta* **1662,** 102–112.
8. Neijssen, J., Pang, B., Neefjes, J. (2007) Gap junction-mediated intercellular communication in the immune system. *Prog. Biophys. Mol. Biol.* **94,** 207–218.
9. Matsue, H., Yao, J., Matsue, K., Nagasaka, A., Sugiyama, H., Aoki, R., Kitamura, M., Shimada, S. (2006) Gap junction-mediated intercellular communication between dendritic cells (DCs) is required for effective activation of DCs. *J. Immunol.* **176,** 181–190.
10. Neijssen, J., Herberts, C., Drijfhout, J. W., Reits, E., Janssen, L., Neefjes, J. (2005) Cross-presentation by intercellular peptide transfer through gap junctions. *Nature* **434,** 83–88.
11. Oviedo-Orta, E., Errington, R. J., Evans, W. H. (2002) Gap junction intercellular communication during lymphocyte transendothelial migration. *Cell Biol. Int.* **26,** 253–263.
12. Oviedo-Orta, E., Gasque, P., Evans, W. H. (2001) Immunoglobulin and cytokine expression in mixed lymphocyte cultures is reduced by disruption of gap junction intercellular communication. *FASEB J.* **15,** 768–774.
13. Wong, C. W., Christen, T., Roth, I., Chadjichristos, C. E., Derouette, J. P., Foglia, B. F., Chanson, M., Goodenough, D. A., Kwak, B. R. (2006) Connexin37 protects against atherosclerosis by regulating monocyte adhesion. *Nat. Med.* **12,** 950–954.
14. Becker, D. L., Evans, W. H., Green, C. R., Warner, A. (1995) Functional analysis of amino acid sequences in connexin43 involved in intercellular communication through gap junctions. *J. Cell Sci.* **108,** 1455–1467.
15. Pearson, R. A., Luneborg, N. L., Becker, D. L., Mobbs, P. (2005) Gap junctions modulate interkinetic nuclear movement in retinal progenitor cells. *J. Neurosci.* **25,** 10803–10814.
16. Kleijmeer, M. J., Morkowski, S., Griffith, J. M., Rudensky, A. Y., Geuze, H. J. (1997) Major histocompatibility complex class II compartments in human and mouse B lymphoblasts represent conventional endocytic compartments. *J. Cell Biol.* **139,** 639–649.
17. Pfaffl, M. W. (2001) A new mathematical model for relative quantification in real-time RT-PCR. *Nucleic Acids Res.* **29,** e45.
18. Musil, L. S., Goodenough, D. A. (1991) Biochemical analysis of connexin43 intracellular transport, phosphorylation, and assembly into gap junctional plaques. *J. Cell Biol.* **115,** 1357–1374.
19. Lin, G. C., Rurangirwa, J. K., Koval, M., Steinberg, T. H. (2004) Gap junctional communication modulates agonist-induced calcium oscillations in transfected HeLa cells. *J. Cell Sci.* **117,** 881–887.
20. Harari, A., Petitpierre, S., Vallelian, F., Pantaleo, G. (2004) Skewed representation of functionally distinct populations of virus-specific CD4 T cells in HIV-1-infected subjects with progressive disease: changes after antiretroviral therapy. *Blood* **103,** 966–972.
21. Bopp, T., Becker, C., Klein, M., Klein-Hessling, S., Palmetshofer, A., Serfling, E., Heib, V., Becker, M., Kubach, J., Schmitt, S., Stoll, S., Schild, H., Staege, M. S., Stassen, M., Jonuleit, H., Schmitt, E. (2007) Cyclic adenosine monophosphate is a key component of regulatory T cell-mediated suppression. *J. Exp. Med.* **204,** 1303–1310.
22. Oviedo-Orta, E., Hoy, T., Evans, W. H. (2000) Intercellular communication in the immune system: differential expression of connexin40 and 43, and perturbation of gap junction channel functions in peripheral blood and tonsil human lymphocyte subpopulations. *Immunology* **99,** 578–590.
23. Bao, X., Lee, S. C., Reuss, L., Altenberg, G. A. (2007) Change in permeant size selectivity by phosphorylation of connexin 43 gap-junctional hemichannels by PKC. *Proc. Natl. Acad. Sci. USA* **104,** 4919–4924.
24. Musil, L. S., Goodenough, D. A. (1990) Gap junctional intercellular communication and the regulation of connexin expression and function. *Curr. Opin. Cell Biol.* **2,** 875–880.
25. Swenson, K. I., Piwnica-Worms, H., McNamee, H., Paul, D. L. (1990) Tyrosine phosphorylation of the gap junction protein connexin43 is required for the pp60v-src-induced inhibition of communication. *Cell Regul.* **1,** 989–1002.
26. Zea, A. H., Rodriguez, P. C., Culotta, K. S., Hernandez, C. P., DeSalvo, J., Ochoa, J. B., Park, H. J., Zabaleta, J., Ochoa, A. C. (2004) L-Arginine modulates CD3ζ expression and T cell function in activated human T lymphocytes. *Cell. Immunol.* **232,** 21–31.
27. Ishii, T., Sugita, Y., Bannai, S. (1987) Regulation of glutathione levels in mouse spleen lymphocytes by transport of cysteine. *J. Cell. Physiol.* **133,** 330–336.
28. Gmunder, H., Eck, H. P., Droge, W. (1991) Low membrane transport activity for cysteine in resting and mitogenically stimulated human lymphocyte preparations and human T cell clones. *Eur. J. Biochem.* **201,** 113–117.
29. Munn, D. H., Shafizadeh, E., Attwood, J. T., Bondarev, I., Pashine, A., Mellor, A. L. (1999) Inhibition of T cell proliferation by macrophage tryptophan catabolism. *J. Exp. Med.* **189,** 1363–1372.
30. Evans, W. H., Boitano, S. (2001) Connexin mimetic peptides: specific inhibitors of gap-junctional intercellular communication. *Biochem. Soc. Trans.* **29,** 606–612.
31. Guan, X., Cravatt, B. F., Ehring, G. R., Hall, J. E., Boger, D. L., Lerner, R. A., Gilula, N. B. (1997) The sleep-inducing lipid oleamide deconvolutes gap junction communication and calcium wave transmission in glial cells. *J. Cell Biol.* **139,** 1785–1792.
32. Mantovani, G., Maccio, A., Madeddu, C., Mura, L., Gramignano, G., Lusso, M. R., Massa, E., Mocci, M., Serpe, R. (2003) Antioxidant agents are effective in inducing lymphocyte progression through cell cycle in advanced cancer patients: assessment of the most important laboratory indexes of cachexia and oxidative stress. *J. Mol. Med.* **81,** 664–673.
33. Kennedy, N. J., Kataoka, T., Tschopp, J., Budd, R. C. (1999) Caspase activation is required for T cell proliferation. *J. Exp. Med.* **190,** 1891–1896.
34. Upham, B. L., Kang, K. S., Cho, H. Y., Trosko, J. E. (1997) Hydrogen peroxide inhibits gap junctional intercellular communication in glutathione sufficient but not glutathione deficient cells. *Carcinogenesis* **18,** 37–42.
35. Gmunder, H., Eck, H. P., Benninghoff, B., Roth, S., Droge, W. (1990) Macrophages regulate intracellular glutathione levels of lymphocytes. Evidence for an immunoregulatory role of cysteine. *Cell. Immunol.* **129,** 32–46.
36. Toyofuku, T., Yabuki, M., Otsu, K., Kuzuya, T., Hori, M., Tada, M. (1998) Intercellular calcium signaling via gap junction in connexin-43-transfected cells. *J. Biol. Chem.* **273,** 1519–1528.
37. Gottesdiener, K. M., Karpinski, B. A., Lindsten, T., Strominger, J. L., Jones, N. H., Thompson, C. B., Leiden, J. M. (1988) Isolation and structural characterization of the human 4F2 heavy-chain gene, an inducible gene involved in T-lymphocyte activation. *Mol. Cell. Biol.* **8,** 3809–3819.
38. Pfeiffer, R., Rossier, G., Spindler, B., Meier, C., Kuhn, L., Verrey, F. (1999) Amino acid transport of y+L-type by heterodimers of 4F2hc/CD98 and members of the glycoprotein-associated amino acid transporter family. *EMBO J.* **18,** 49–57.
39. Verma, V., Hallett, M. B., Leybaert, L., Martin, P. E., Evans, W. H. (2009) Perturbing plasma membrane hemichannels attenuates calcium signaling in cardiac cells and HeLa cells expressing connexins. *Eur. J. Cell Biol.* **88,** 79–90.
40. Oelze, I., Kartenbeck, J., Crusius, K., Alonso, A. (1995) Human papillomavirus type 16 E5 protein affects cell–cell communication in an epithelial cell line. *J. Virol.* **69,** 4489–4494.

KEY WORDS:
connexin 43 · T cell receptor · hemichannels · cysteine uptake · cell cycle · lymphocytes · gap junction